Earthquake Resistance of Transmission Steel Towers

Yusuke Sato
Central Research Institute of Electric Power Industry (CRIEPI), Chiba, Japan

Tomomi Ishikawa
Central Research Institute of Electric Power Industry (CRIEPI), Chiba, Japan

SUMMARY:
This paper discusses earthquake resistance of transmission steel towers with comparative analyses of wind resistance data. For this purpose, we conducted large deformation and elasto-plastic analyses. The target tower was of a square configuration constructed of steel pipe members. The analyses considered a wind load with a design wind velocity of 40m/s and the ground motion observed in the 1995 Kobe Earthquake. The peak acceleration of the input earthquake data was adjusted to a value determined under the assumption that the maximum top displacement is the same in the linear analyses for both earthquake and wind responses. Results showed that the peak axial forces remained under the buckling strength of the main leg members in the seismic analysis, but that buckling occurred at the lowest panel in the wind response analysis. These results demonstrate that the earthquake resistance margin of the target tower is greater than the wind resistance margin.

Keywords: transmission steel tower, earthquake resistance, large deformation and elasto-plastic analysis

1. INTRODUCTION

Even though Japan has experienced some of the world's largest earthquakes in recent years, notably the Kobe Earthquake in 1995 and the Tohoku Earthquake in 2011, there has been no record of a transmission steel tower collapsing because of seismic motion. However, during the 1995 Kobe Earthquake, the occurrence of an elastic response to ground motions on a tower was identified by a seismic response analysis.

There is a possibility that some plastic tower response occurred during the Tohoku earthquake since peak ground accelerations (PGA) there were larger than those observed in the Kobe earthquake, but seismic resistance considering plastic response during a major earthquake was not estimated because transmission steel towers are designed for wind resistance and the nonlinear behaviour of transmission steel towers during a seismic event has not yet been sufficiently investigated. Therefore, it is important to identify the limit state of transmission steel towers in order to provide protection against future giant earthquakes. In the present study, earthquake resistance of transmission steel towers is discussed with a comparative analysis of wind resistance data.

2. FINITE ELEMENT ANALYSIS CONDITIONS

We conducted a finite element analysis (FEA) using the general purpose commercial code ABAQUS in order to evaluate the limit state of the steel tower. In the following section we describe the FEA model, the material conditions and the load conditions.

2.1. Finite element analysis model

Figure 1 shows the target tower which is a 500 kV tension square tower with steel pipe members and with a height of 75.5m. The target tower was modelled as a nonlinear beam element. Cables were idealized as a mass element because the interaction between the tower and overhead wires was disregarded in order to specifically investigate the tower's nonlinear response. All members were divided into five elements. The number of nodes and elements of the FEA model was 7,471 and 3,994, respectively.

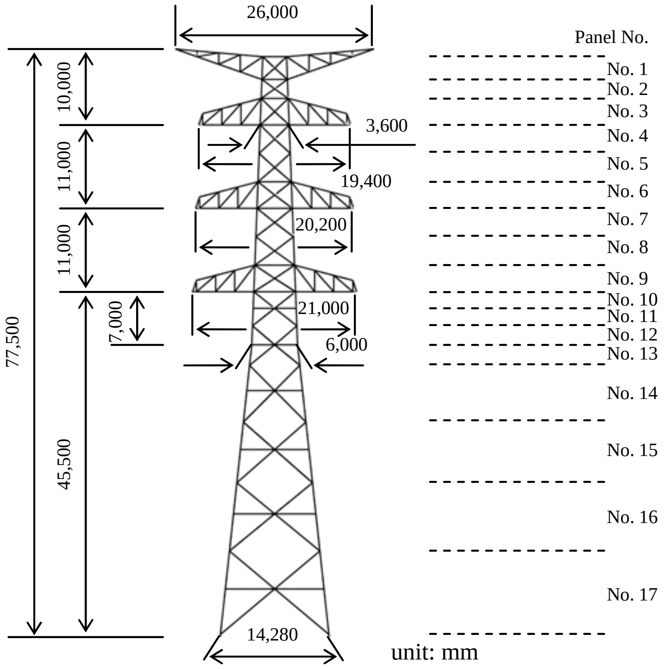

Figure1. Target tower

2.2. Material conditions

The relationship between strain and stress was modelled as a bi-linear curve. Figure 2 shows the material characteristics used in this analysis. The Young modulus was 206,000MPa and the yield stress was 229 MPa. A second slope of the bi-linear curve was 1% of the Young modulus and a kinematic hardening rule was applied. Poisson's ratio and the density were 0.3 and 7.87t/m^3, respectively. Damping was assumed to be proportional to the stiffness. The damping ratio was equal to 0.01% for the first mode of the tower.

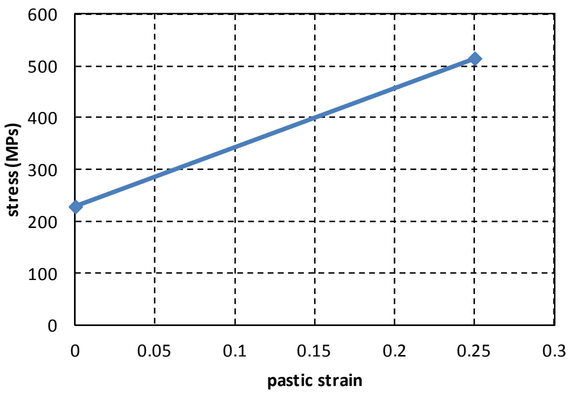

Figure2. Material characteristic

Each mass of the overhead wires and tension insulator assemblies was shown in Table1. When mass of the overhead wires was decided, it was assumed that span length between towers was equal to 450m and each arm of the tower supported a half of the wires mass.

Table 1. Overhead wires and tension insulator assembly mass

	Mass per unit length (kg/mm)	Cross section (mm^2)	Young's modulus (MPa)	Mass (kg)
Ground wire	0.0108	3484	71.10	558
Conductor	0.00124	263.2	103.0	4860
Tension insulator assembly	0.1926	660	115.2	763

2.3. Load conditions

In order to compare seismic and wind response of the target tower, seismic and wind loads were applied as external loads and the load conditions are described below.

2.3.1. Earthquake

An EW component of the observed ground motion at Kobe, where the Japan Meteorological Agency maintained an observation site during the 1995 Kobe Earthquake (hereafter referred to as JMA Kobe), was used as the input seismic motion. The acceleration time history and the acceleration response spectrum of JMA Kobe are shown in Figure 3 and Figure 4, respectively. This analysis considers the line-cross direction for the seismic input. The maximum acceleration of JMA Kobe was 617 Gal.

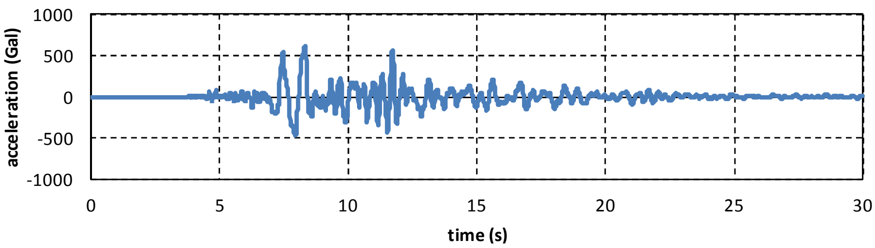

Figure3. Ground motion record (JMA Kobe, EW component)

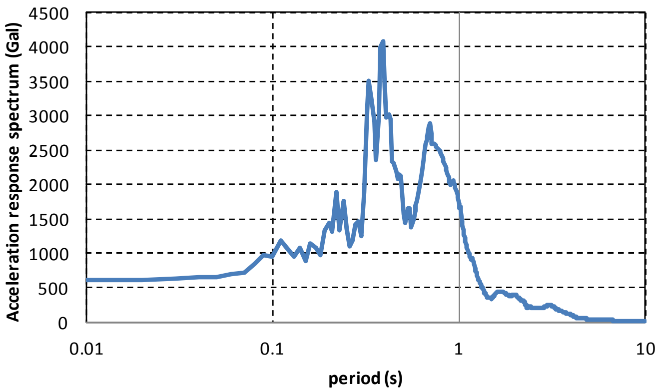

Figure4. Acceleration response spectrum of JMA Kobe (h=0.01)

2.3.2. Wind load

The design wind velocity was equal to 40m/s at 10m height with roughness category III. In general, the wind load was defined as follows:

$$f = \frac{1}{2}\rho C_d A\bar{U}^2 + \rho CdA\bar{U}u(t) \tag{2.1}$$

where ρ was an air density, C_d was a coefficient of wind force, A was a wind receiving area, $\bar{U}$ was an average wind velocity and $u(t)$ was a fluctuating wind velocity.

Table 2 shows the average wind velocities, coefficients of wind force and wind receiving areas for each panel of the tower. The fluctuating wind velocities were assumed based on a method proposed by

Yamazaki, M. et al. The fluctuating wind velocities of the tower top and lowest panel are shown in Figure 5. The dynamic wind loads were calculated based on the assumed fluctuating wind velocities with the condition that each span length in front of and behind the target tower was equal to 450m.

Table2. Parameter for average wind load calculation

Panel number	average wind velocity (m/s)	coefficient of wind force	wind receiving area (mm^2)
1 (tower body)	47.52	1.966	1.576
1 (arm)	47.52	2.596	3.494
2	47.167	1.977	1.344
3 (tower body)	46.768	1.912	2.474
3 (arm)	46.768	2.354	3.819
4	46.268	1.952	2.518
5	45.727	1.884	3.321
6 (tower body)	45.178	1.873	3.406
6 (arm)	45.178	2.395	3.634
7	44.601	1.913	3.451
8	43.971	1.925	3.523
9 (tower body)	43.326	1.908	3.652
9 (arm)	43.326	2.387	3.66
10	42.579	1.868	5.565
11	41.587	1.93	5.883
12	40.191	1.966	8.998
13	38.048	2.01	10.05
14	34.976	2.05	11.53
15	28.955	2.083	14.48

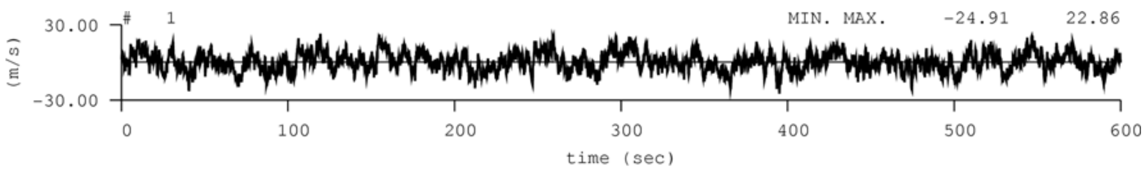

(a) Top

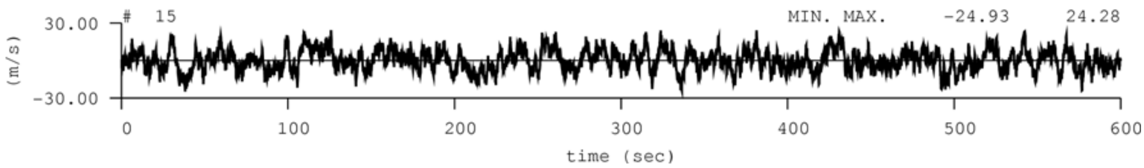

(b) Lowest panel

Figure5. Fluctuating wind velocity of the tower top and lowest panel

3. RESULTS AND DISCUSSIONS

The dynamic analyses for the finite element model of the target tower were conducted. In the following, the mode analysis results, determination of the relationship between seismic and wind load, the wind response analysis results and the seismic response analysis results are described.

3.1. Mode analysis

Mode shapes and natural frequencies for the respective modes of the target tower are shown in Figure 6, in which the first and second modes for line and line-cross directions are depicted. The first natural frequencies are 1.56Hz and 1.54Hz for line and line-cross directions, respectively.

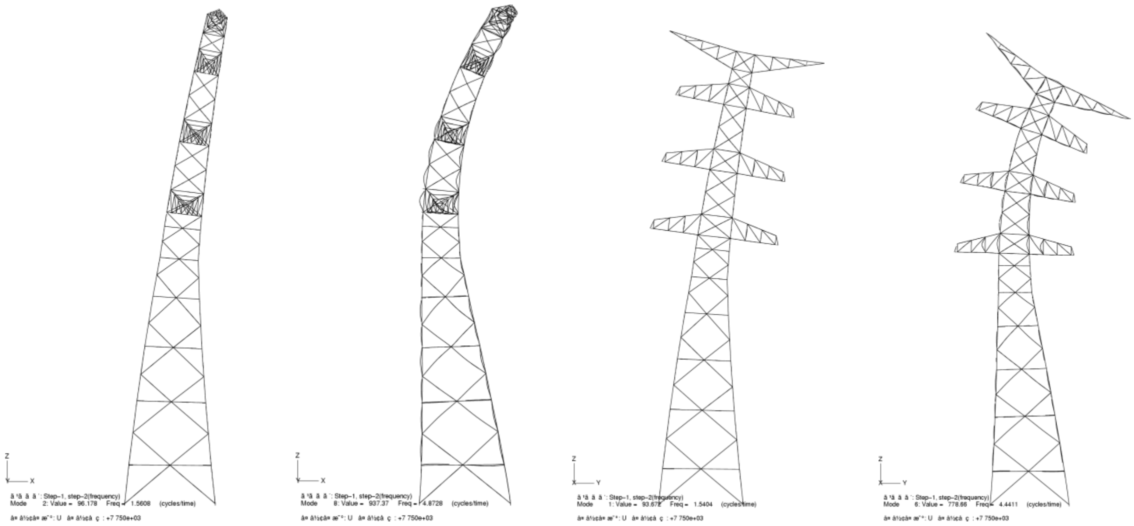

(a) line direction first mode (1.56Hz) (b) line direction second mode (3.56Hz) (c) line-cross direction first mode (1.54Hz) (d) line-cross direction second mode (3.06Hz)

Figure6. Mode shapes and natural frequencies of the target tower

3.2. Relationship between earthquake and wind load

In order to compare the wind and earthquake response, a peak acceleration of input earthquake was adjusted as follows:

A linear dynamic analysis was conducted using the original JMA Kobe record and wind load which are described in 2.3.2. The maximum displacement of the tower top was then identified. The peak acceleration of the input seismic data was adjusted to a value determined under the assumption that the maximum displacement of the tower top is the same in the linear analyses for both earthquake and wind responses. The maximum displacement of the tower top was 587.6mm in the seismic analysis and 991.8mm in the wind response analysis, thus leading us to conclude that the peak acceleration of the input earthquake data was approximately 1.7 times as large as that of the original JMA Kobe record.

3.3. Wind response analysis results

The nonlinear wind response analysis has not been completed due to the large deformation of the tower members. Figure 7 shows the deformation and the distribution of the von Mises stress and the equivalent plastic strain at the moment of the last step. The maximum displacement of the tower top was 3,965mm. The large deformation of the lowest panel members on the compression side occurred due to plastic buckling.

Figure 8 shows the ratio of the maximum axial force of the main and brace members for each panel to the tolerance levels, namely the buckling load and tension yield stress. The ratios of the main and brace members at the lowest panel on the compression side are smaller than that of the other members. The ratios of the panels not plotted in Figure 7 were more than 5.

3.4. Seismic response analysis

The displacement and acceleration time histories of the tower top in the nonlinear seismic analysis are shown in Figure 9 and Figure 10, respectively. The maximum top displacement of 692.8mm was less than about one fifth of that in the wind response analysis. The residual deformation of the top was equal to about 46mm. The maximum acceleration of 2,608mm/s^2 was about 2.5 times as large as the maximum acceleration of the earthquake input, which was 1,043Gal.

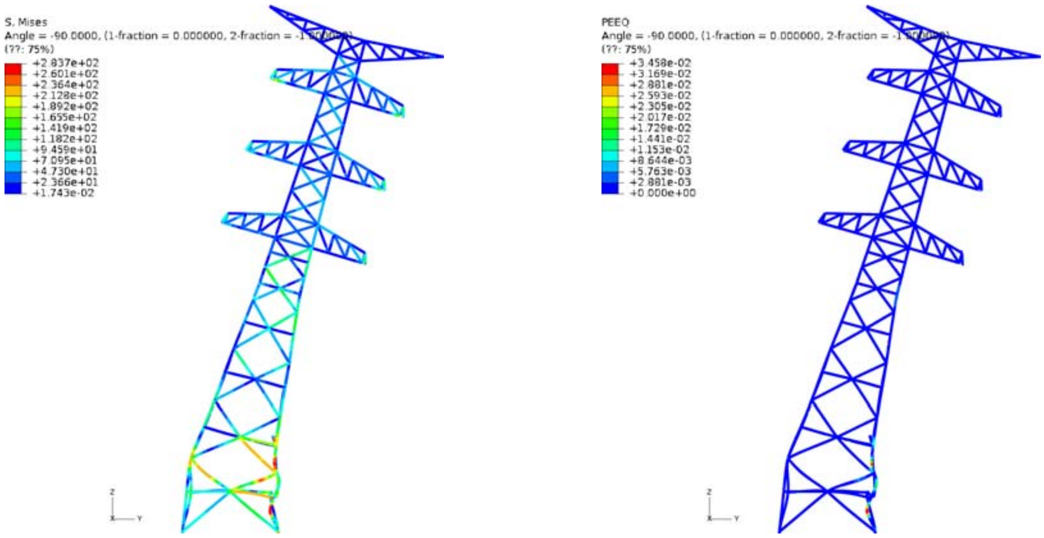

(a) von Mises stress (unit: MPa) (b) equivalent plastic strain

Figure7. Deformation at last step (wind response analysis, deformation magnification 5 times)

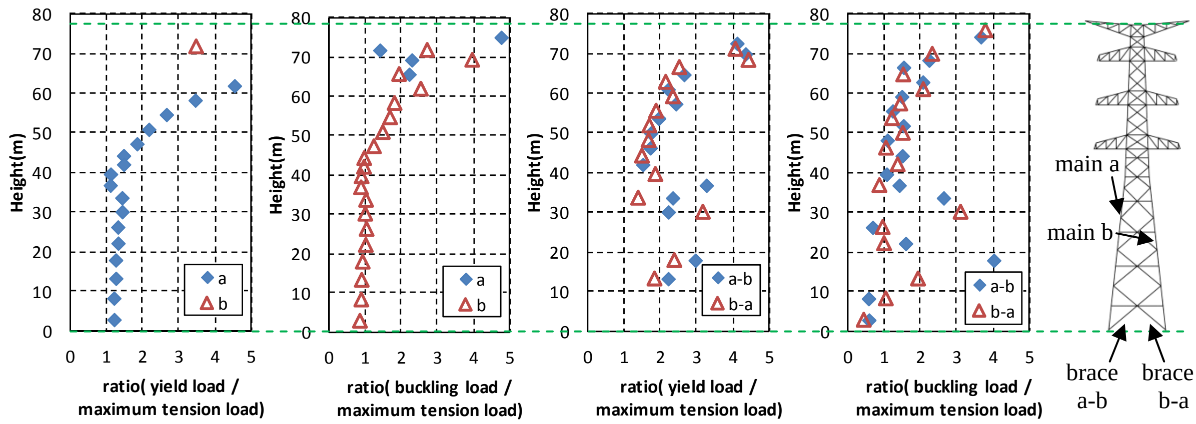

(a) tension load (main member) (b) compression load (main member) (c) tension load (brace member) (d) compression load (brace member)

Figure8. Maximum tension and compression axial forces for each panel (wind response analysis)

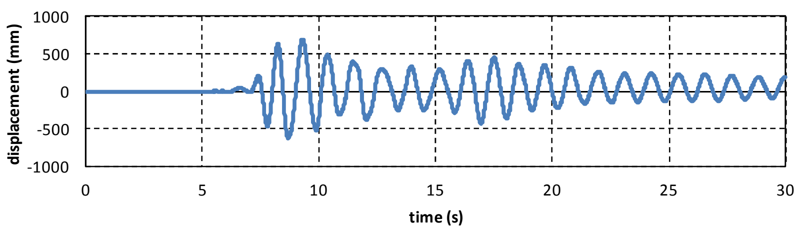

Figure9. Displacement time history of the tower top (seismic response analysis)

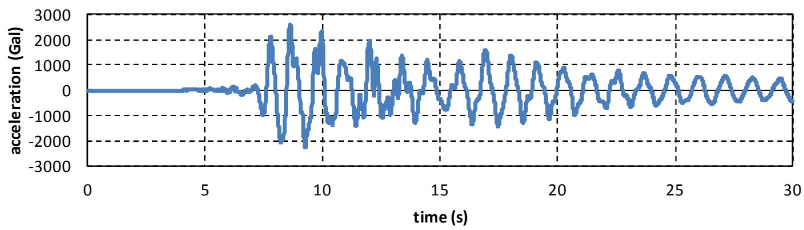

Figure10. Acceleration time history of the tower top (seismic response analysis)

Figure 11 shows the deformation and the distribution of the von Mises stress and the equivalent plastic strain at the moment maximum displacement was reached. Buckling deformation occurred on one of the brace members on the third panel.

Figure 12 shows the ratio of the maximum axial force of the main and brace members of each panel to the tolerance levels. In the seismic analysis, the panels that support the cross-arm, the 3rd, 6th and 9th panels, showed a ratio of less than 1.0 while the main leg members of the peak axial forces remained below the buckling strength of the lowest main leg member.

These results suggest the earthquake resistance margin of the target tower was greater than the wind resistance margin.

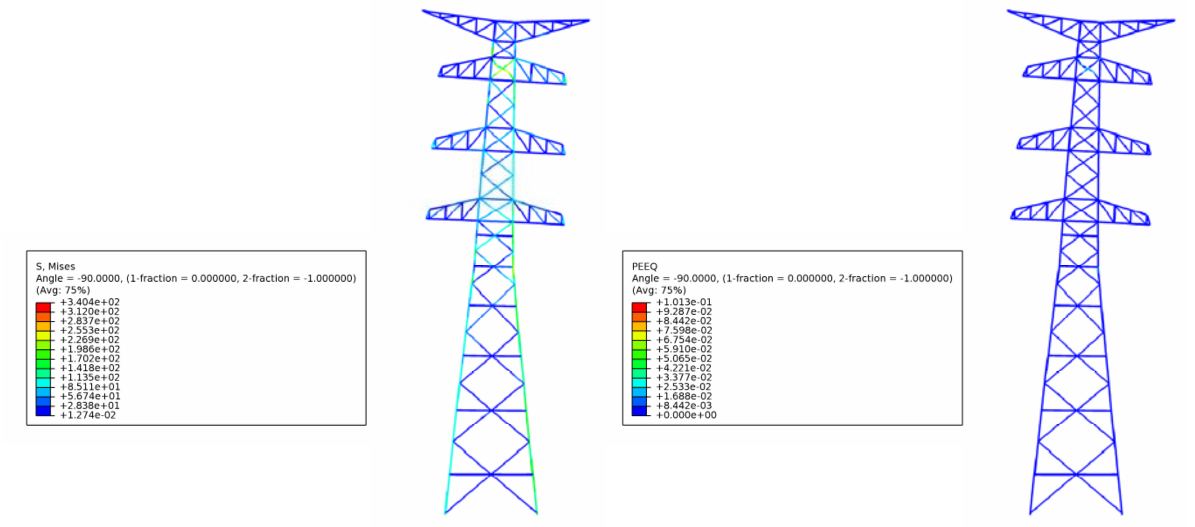

(a) von Mises stress (unit: MPa) (b) equivalent plastic strain

Figure11. Deformation at the moment maximum displacement was reached (seismic response analysis, deformation magnification 5 times)

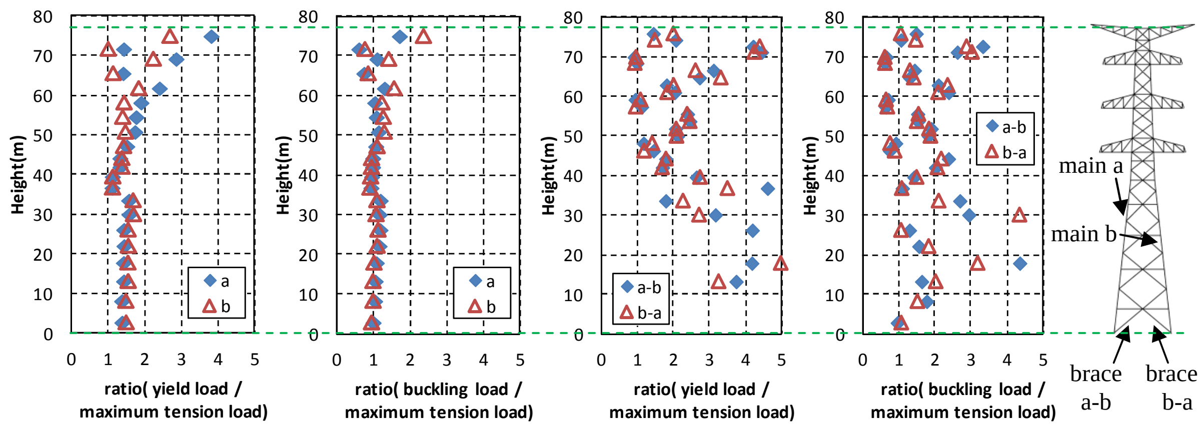

(a) tension load (main member) (b) compression load (main member) (c) tension load (brace member) (d) compression load (brace member)

Figure12. Maximum tension and compression axial forces for each panel (seismic response analysis)

4. CONCLUSIONS

This study examined the earthquake resistance of transmission steel towers with a comparative analysis of wind resistance data. Based on the results of the seismic response analysis and wind response analysis, we were able to make the following conclusions:

(1) In order to compare seismic response to wind response, we conducted a linear seismic analysis with input from the original JMA Kobe and the linear wind response analysis with a design wind velocity of 40m/s at 10m height and roughness category III. The maximum displacement of the tower top in the seismic analysis was less than 0.6 times that in the wind response analysis.

(2) The large deformation and elasto-plastic dynamic analyses were conducted using a wind load and earthquake data with peak acceleration approximately 1.7 times that of the original JMA Kobe record based on the linear analysis. The maximum displacement of the tower top in the nonlinear seismic analysis was equal to about one fifth of that in the nonlinear wind response analysis. Moreover, the peak axial forces remained below the buckling strength of main leg members in the seismic analysis while buckling occurred on the lowest main leg member in the wind response analysis. These results suggest that the earthquake resistance margin of the target tower is greater than the wind resistance margin.

REFERENCES

The Japanese Electrotechnical Committee (1980). Design Standards on Structures for transmissions (JEC-127), Denkishoin

Transmission expert Committee (2008). Overhead Transmission Line Code (JEAC 6001-2008), The Japan Electric Association

SIMULIA (2007). ABAQUS User’s Manual Version6.9

Yamazaki, M., Ishikawa, T., Ohkuma, T., Tamura, Y., Kitashima, T., Nakamura, H. and Kato, H. (2004). A study on directional basic wind speed for the wind resistant design of transmission tower (in Japanese). *Journal of Wind Engineering* **Vol29: No.3**, 19-34